Journal of Magnetism and Magnetic Materials 427 (2017) 14–18

Contents lists available at ScienceDirect

Journal of Magnetism and Magnetic Materials

journal homepage: www.elsevier.com/locate/jmmm

Sensitive magnetic biodetection using magnetic multi-core nanoparticles and RCA coils

Fredrik Ahrentorp[a], Jakob Blomgren[a], Christian Jonasson[a], Anna Sarwe[a], Sobhan Sepehri[b], Emil Eriksson[b], Alexei Kalaboukhov[b], Aldo Jesorka[b], Dag Winkler[b], Justin F. Schneiderman[c], Mats Nilsson[d], Jan Albert[e,f], Teresa Zardán Gómez de la Torre[g], Maria Strømme[g], Christer Johansson[a,*]

[a] Acreo Swedish ICT AB, Arvid Hedvalls Backe 4, Göteborg, Sweden
[b] Department of Microtechnology and Nanoscience – MC2, Chalmers University of Technology, Göteborg, Sweden
[c] Institute of Neuroscience and Physiology, University of Gothenburg and MedTech West, Göteborg, Sweden
[d] Science for Life Laboratory, Department of Biochemistry and Biophysics, Stockholm University, Stockholm, Sweden
[e] Department of Microbiology, Tumor and Cell Biology, Karolinska Institutet, Stockholm, Sweden
[f] Department of Clinical Microbiology, Karolinska University Hospital, Stockholm, Sweden
[g] Uppsala University, Uppsala, Sweden

ARTICLE INFO

Keywords:
Magnetic nanoparticles
Magnetic multi-core particles
AC susceptometry
RCA coil
Differential induction coil
Biodetection

ABSTRACT

We use functionalized iron oxide magnetic multi-core particles of 100 nm in size (hydrodynamic particle diameter) and AC susceptometry (ACS) methods to measure the binding reactions between the magnetic nanoparticles (MNPs) and bio-analyte products produced from DNA segments using the rolling circle amplification (RCA) method. We use sensitive induction detection techniques in order to measure the ACS response. The DNA is amplified via RCA to generate RCA coils with a specific size that is dependent on the amplification time. After about 75 min of amplification we obtain an average RCA coil diameter of about 1 μm. We determine a theoretical limit of detection (LOD) in the range of 11 attomole (corresponding to an analyte concentration of 55 fM for a sample volume of 200 μL) from the ACS dynamic response after the MNPs have bound to the RCA coils and the measured ACS readout noise. We also discuss further possible improvements of the LOD.

1. Introduction

Magnetic multi-core iron oxide based nanoparticles (magnetic nanoparticles, MNPs) are used for a variety of biomedical applications such as diagnostics, therapy, actuation and imaging [1,2]. Several biomolecular sensing platforms based on magnetic detection of functionalized MNPs have been reported [2–9]. Such methods quantify (i) changes to the magnetic properties of the fluid-suspended MNP ensemble when biomolecular binding events occur between the MNPs and the analyte and/or (ii) the presence of stray magnetic fields originating from MNPs bound via the analyte to a sensing area. Herein, we present a highly sensitive magnetic biosensing approach based on functionalized iron oxide based magnetic multi-core particles and AC susceptometer (ACS) methods to measure the binding reaction between MNPs and the bio-analyte product. Our target bio-analyte is influenza virus RNA strands from nasopharyngeal samples. To limit health related consequences, rapid, sensitive and specific diagnostic assays are critical to enable adequate patient care. A reliable and sensitive assay with a short turn-around-time (TAT) for detecting influenza-infections in respiratory samples is thus highly desirable. Current influenza tests are typically PCR-based and have a TAT of several hours and are performed in dedicated bioanalytical laboratories. This assay instrumentation is relatively large and expensive, and is therefore not available at the point of care or in smaller emergency wards.

We develop a low-cost and portable diagnostics unit for rapid detection of seasonal and pandemic influenza virus. This portable sensing solution aims at shortening TAT to < 60 min, while still retaining high analytical sensitivity. The methods and instruments developed in the project focus on influenza, but are generic and not limited to this specific disease. In the final detection system we will integrate both the fluidic system that handles sample preparation and

* Corresponding author.
E-mail address: christer.johansson@acreo.se (C. Johansson).

http://dx.doi.org/10.1016/j.jmmm.2016.10.041
Received 26 June 2016; Received in revised form 18 September 2016; Accepted 8 October 2016
Available online 10 October 2016
0304-8853/

actuation with the magnetic detection method; all elements in the system will be software controlled. We compare and validate two detection methods: induction differential coils and a superconducting sensor. All sample-handling steps of the bioassay in the final device will be performed on a disposable lab-on-a-chip system.

We have previously demonstrated that ACS-based bio-detection of MNPs can be made portable with high sensitivity [9]. The detection principle relies on measurements of the changes in Brownian relaxation of suspended oligonucleotide-functionalized MNPs including volume amplification of the bioanalyte (in this case cDNA target) using the padlock-probe-ligation technique and rolling circle amplification (RCA) [4,5,9–11]. The obtained RCA coils are in the size range of 1 μm (for RCA amplification time of 75 min). The exchange between the initial number of DNA segments and the number of RCA coils is 1:1, meaning that the number of DNA segments is equal to the number of RCA coils. This can be further improved by using an additional RCA coil amplification but this will increase the TAT.

Our induction-based technique is based on the DynoMag system [4,9]. We also use as magnetic readout a high critical temperature superconducting quantum interference device (high-T_c SQUID) gradiometer [11]. In this article we will only present the result from the induction based technique. In an upcoming publication we will present more about the high-T_c SQUID used in this biodetection application.

2. Experimental

2.1. Materials and methods

The magnetic readout is based on a frequency-swept measurement of the in- and out-of-phase components of the MNP ensemble ACS from which we extract the Brownian relaxation frequency [12]. The MNP system used in this study was composed of suspended iron oxide based multi-core particles with a mean hydrodynamic particle size of 100 nm (Micromod Partikeltechnologie GmbH). The individual magnetic cores in the particles are in the range of 10–20 nm. The effective relaxation of the MNPs is a combination of the Néel relaxation and the Brownian relaxation but the relaxation process will be dominated by the shortest relaxation time. For this particular MNP system the Néel relaxation time is longer than the Brownian relaxation and thus the MNPs will exhibit Brownian relaxation and dominate the ACS dynamics in the frequency window of the detection system (1–10000 Hz). The Brownian relaxation frequency, f_B, can be described by:

$$f_B = \frac{k_B T}{6\pi\eta V_H} \tag{1}$$

where k_B is Boltzmann's constant, T the temperature, η the viscosity of the carrier liquid, and V_H the hydrodynamic volume of the MNP. The Brownian relaxation frequency can be approximately identified as the frequency where the out-of-phase component in the AC susceptibility is at its maximum; it is furthermore sensitive to changes in the MNP hydrodynamic volume, which in turn increases when the MNPs bind to target molecules. We have previously shown that ACS can be used as a biodetection technique by measuring changes in the Brownian relaxation frequency due to direct binding reactions of biomolecules to the surfaces of the MNPs [4]. The analyte sensitivity was found to be in the nM range. The method was further improved in terms of sensitivity (sub-pM range), by amplifying the bioanalyte using the RCA-technique to build up large RCA coil molecules [5,10] where the shift in Brownian relaxation is much larger when the binding occurs. These RCA coils are produced in a series of reactions that start with target recognition using padlock probes. Padlock probes are short oligonucleotides with ends designed to hybridize specifically with a target DNA sequence. The ends of the probes are joined by ligation to form a DNA circle. The circular probes are suitable templates for RCA, and this technique is used for creating long DNA coils that collapse into micrometer-sized DNA products. The padlock probes are hybridized and ligated, templated by the target at 37 °C for 15 min. The ends of the probes are joined by ligation to form a DNA circle. The circular probes are then amplified at 37 °C for 1 h, followed by enzymatic inactivation at 65 °C for 5 min. The method is equally applicable to the influenza RNA we aim to detect herein. We have previously shown the increase in sensitivity using this RCA -coil/MNP technique [5,9], and sensitivity could be increased to the sub-pM range (and can be even further improved). In this method the initial DNA segments are amplified in the RCA-coil process [5,10] building up RCA-coils with a size of 1 μm in about 75 min.

Hybridization between MNPs and RCA coils (about 20 min) results in a dramatic increase in the hydrodynamic size of the MNPs. This causes a decrease in the relaxation frequency of the MNPs from ~100 Hz (free MNPs) to ~1 Hz (MNPs bound to RCA coil). This frequency shift thus confirms the presence of target molecules. The concentration of target molecules can also be monitored as a corresponding decrease of the amplitude of the Brownian relaxation peak of free MNPs. Such a reduction of the peak signal of the out-of-phase component of the AC susceptibility is our primary bio-detection parameter. The obtained ACS relaxation at low frequencies (1 – 20 Hz) is due to the Brownian relaxation of the MNP/RCA coils, since the measured Néel relaxation time for the individual magnetic cores when immobilizing the MNPs [13] is longer as compared with the low frequency Brownian relaxation time for RCA coils in the size range of 1 μm.

Fig. 1 shows the Acreo DynoMag differential induction based detection system.

The DynoMag system measures the in-phase (real part) and out-of-phase-component (imaginary part) of the AC susceptibility versus excitation frequency in the range of 1 Hz–500 kHz. The system comprises two well balanced differential pick-up coils centered in an excitation coil (see Fig. 2). The excitation coil is connected to an AC source that delivers the current that produces the AC field that magnetizes the sample. The pick-up coil is connected to a lock-in amplifier that detects the differential voltage from the coils. The in- and out-of-phase components of this differential voltage are directly related to the out-of-phase and in-phase components of the AC susceptibility, respectively. The relation between the voltage and AC susceptibility (AC magnetic moment) is calibrated with a paramagnetic substance (Dy_2O_3) in the full frequency range.

The sample is measured both in the lower and the upper position in the pick-up coil in order to reduce the background signal. In the DynoMag system this is achieved by using a stepper motor for actuation of 200 μL sample volumes. In this project, we will modify the DynoMag sample handling system for a reduced detection volume of about 50 μL. A polymer tube is inserted through the detection coil and a plug-flow technique with a pump serves to move the sample.

Fig. 1. The figure shows the Acreo DynoMag system including the integrated electronics with the coil system (excitation and detection, inside the aluminum box) and the dedicated software that controls the measurement and performs the magnetic analysis.

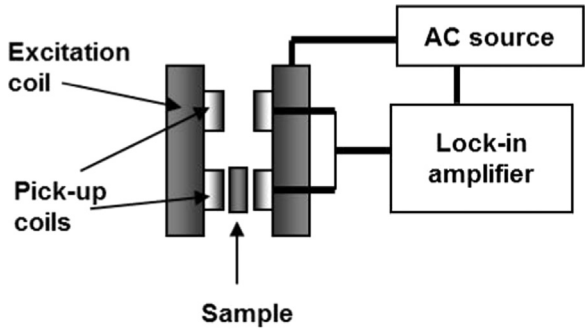

Fig. 2. Schematic picture of the excitation coil, the pick-up coils, AC source, and lock-in amplifier that is integrated in the DynoMag system shown in Fig. 1.

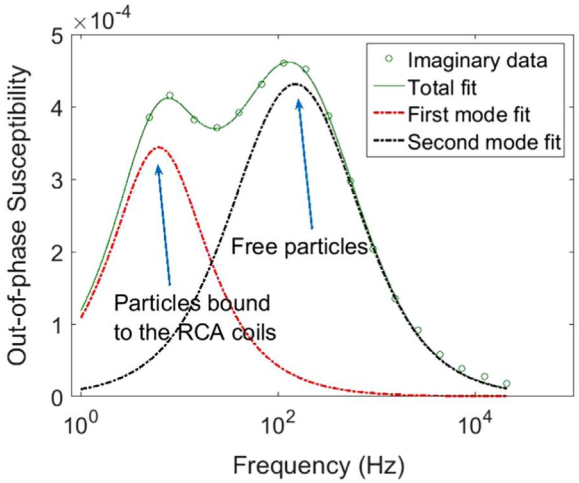

Fig. 3. The out-of-phase component (imaginary part) of the ACS signal versus frequency when the MNPs bind to RCA coils. The out-of-phase component relaxation peak at 100 Hz corresponds to the free (unbound) MNPs. At lower frequencies (around 1 Hz) a relaxation peak builds up corresponding to MNPs that are bound to the RCA coils. The solid line is the result of fitting the ACS spectra with the bi-modal Brownian relaxation model described in the text.

In Fig. 3 we present an example of the ACS out-of-phase component versus frequency when the MNPs bind to the RCA coils. The relaxation peak at about 100 Hz is due to the free MNPs that have not bound to the RCA coils and the low frequency relaxation that is building up at about 1 Hz corresponds to the ACS response from MNPs that have bound to the RCA coils.

In order to find the peak signal in an accurate way from discrete experimental data points we use a bi-modal Brownian relaxation model that takes into account both the free MNPs (at around 100 Hz) and the bound MNPs (at around 1 Hz). In this case we choose a Cole-Cole relaxation superposition model for both the low and high frequency relaxation. The AC susceptibility, $\chi(\omega)$, can then be expressed as:

$$\chi(\omega) = \frac{\chi_{01}}{1 + (j\omega\tau_1)^{\alpha_1}} + \frac{\chi_{02}}{1 + (j\omega\tau_2)^{\alpha_2}} + \chi_{high} \quad (2)$$

where the first part handles the relaxation at low frequencies (bound MNPs) and the second part handles the relaxation at higher frequencies (free MNPs). In Eq. 2, $\omega=2\pi f$ where f is the frequency, α_1 and α_2 are phenomenological width parameters of the two relaxation distributions (for the bound and free MNPs), τ_1 and τ_2 are the relaxation times of each relaxation, and χ_{high} is the high frequency contribution to the in-phase component. The solid line in Fig. 3 is a result of fitting the measured data to this model.

The limit of detection value (LOD) can be written as

$$LOD = \frac{\chi''_{noise}}{C^* g_{RCA}{}^* g_{MNP}} \quad (3)$$

where, χ''_{noise} is the out-of-phase susceptibility noise of the detection system, C is the out-of-phase susceptibility per MNP of the particle system, g_{RCA} is the number of RCA coils generated from each target molecule, and g_{MNP} is the number of MNPs bound to each RCA coil. The signal noise χ''_{noise} is obtained from the standard deviation value of the out-of-phase component measured at the relaxation peak frequency on a sample with the initial MNP concentration (particle mass concentration 0.1 mg/mL).

2.2. Experimental results

In Fig. 4a and b we show the result of the measured in- and out-of-phase ACS components versus frequency for different concentrations of RCA coils (produced from rolling circular amplifications of synthetic *Vibrio cholera* target DNA) measured with the DynoMag system. Negative sample data (zero RCA coil concentration) are also included.

As can be seen in Fig. 4a and b the ACS signal in the range of 10 Hz–100 Hz in both the in-phase and out-of-phase components decrease when the RCA coil concentration increases. This is because the number of free MNPs decreases as the number/concentration of RCA coils (and subsequent binding events) increases. It is interesting to see from Fig. 4b that the Brownian relaxation peak increases in frequency with increasing RCA coil concentration. This means (when studying the earlier given expression for the Brownian relaxation

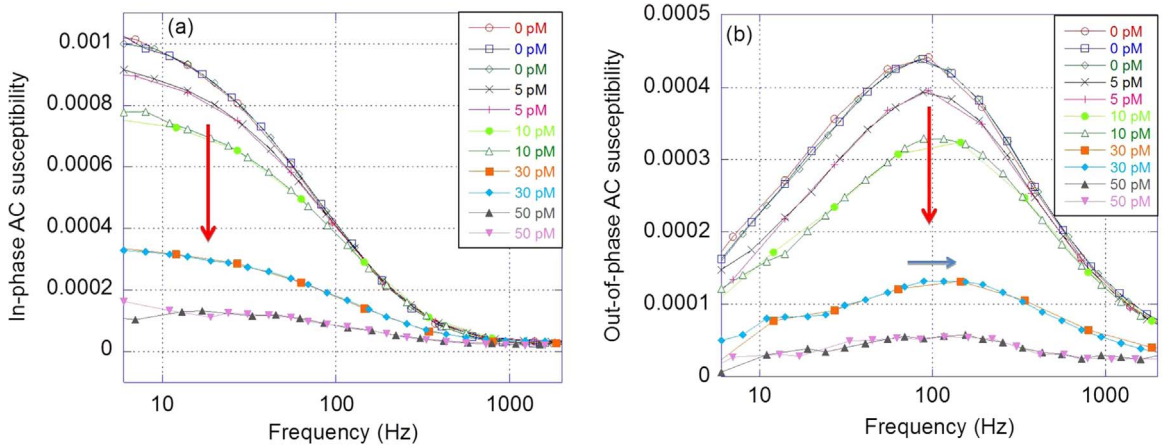

Fig. 4. In- (real, a) and out-of-phase (imaginary, b) components of the ACS signal versus frequency for different concentrations of RCA coils (from 0 pM to 50 pM). The AC susceptibility is given as volume susceptibility (SI units). Red arrows indicate the decrease in amplitude of both components as the number of free particles bound to the RCA coils increases. In b), the out-of-phase component peak frequency also shifts to higher frequency as binding events occur, suggesting larger MNPs bind more easily to the RCA coils. (For interpretation of the references to color in this figure legend, the reader is referred to the web version of this article.)

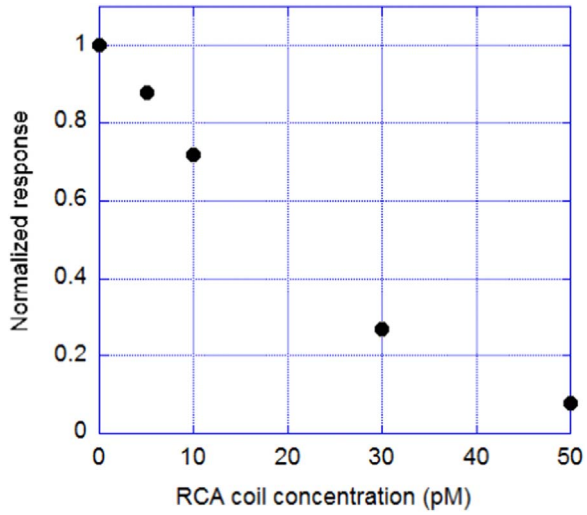

Fig. 5. Normalized response curve (peak signal of the out of phase component normalized to the value of the negative sample) versus concentration of the RCA coils.

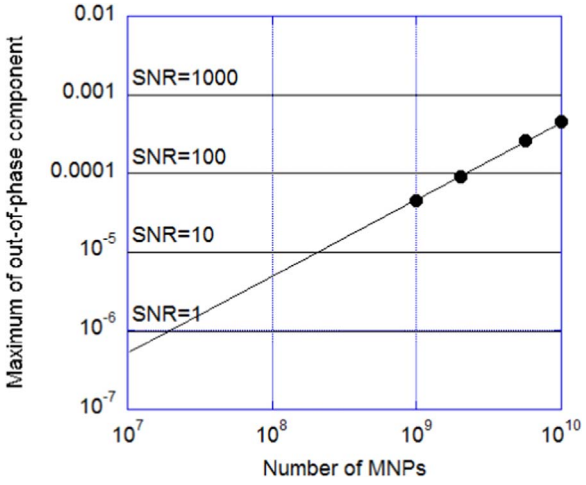

Fig. 6. Peak signal of the out-of-phase component versus number of MNPS in the sample. The sample volume used here is 200 μL measured with the DynoMag system. In the figure also the signal to noise ratios (SNR) are shown.

frequency, Eq. (1)) that the larger MNPs in the ensemble bind more easily to the RCA coils. In the MNP system we have a distribution of hydrodynamic particle sizes from about 75 nm and 125 nm (size distribution width given as the sigma value in log-normal distributed sizes).

We extract a response curve for our detection principle from a slice of the out-of-phase data at the peak signal (~100 Hz, marked by the red arrow in Fig. 4b). In Fig. 5, we present the peak signal of the out-of-phase component as a function of RCA coil concentration. The values are normalized to the peak signal for the negative sample (zero RCA coil concentration).

The system response is close to linear for RCA coil concentrations below ~30 pM. At higher RCA coil concentrations the response levels out presumably because a larger fraction of RCA coils are required in order to bind the remaining free MNPs.

We furthermore estimate the mean value of the number of MNPs that bind to each RCA coil from: 1) the ACS signal of the negative sample (zero RCA coil concentration), 2) the magnitude of the out-of-phase component as a function of RCA coil concentration, 3) the initial particle number concentration (particle mass concentration of 0.1 mg/mL) and 4) the sample volume. For this experiment, we obtain a mean value of about 3 MNPs per RCA coil.

To find a theoretical estimation of the LOD, we link the number of target molecules in the sample to the measured shift in the susceptibility and compare this with the sensitivity of the instrument (the noise in the ACS signal). In Fig. 6 we plot the peak ACS signal versus the number of MNPs in the sample for the DynoMag measurements (sample volume of 200 μL). In the figure we have also given the signal to noise ratios (SNR).

From such a measurement we get a standard deviation value of $\chi''_{noise}=10^{-6}$ given as volume susceptibility. This value corresponds to a SNR of 1 and in turn indicates a detection limit of about 2×10^{7} MNPs (in a sample volume of 200 μL).

3. Discussion

The mean value of MNPs bound to each RCA coil is quite low when considering the size of the RCA coils (1 μm) as compared to that of the MNPs (100 nm). Such a low value can be attributed to a limited number of binding sights per RCA coil. Future work will include modifying the RCA chemistry in order to boost the number of available binding sites per coil.

If 3 MNPs binds to each RCA coil ($g_{MNP}=3$) and since we have 1:1 exchange between initial DNA segments and RCA coils ($g_{RCA}=1$), then we can detect RCA coils with a LOD of 11 attomoles that corresponds to a concentration in the range of 55 fM (theoretical estimated LOD determined from the ACS noise). We will continue to measure on lower RCA coil concentrations down to the fM range in order to experimentally demonstrate the absolute LOD and to better understand the response curve.

4. Conclusions

We have shown the development of a biodetection system using a functionalized MNP system (multi-core particles, 100 nm in size) and ACS methods to measure the change in Brownian relaxation properties induced by binding to RCA coils. The biodetection analyte in the final device is RNA extracted from influenza virus. The transformed DNA segments (cDNA) are amplified using the RCA technique to build RCA coils in the size range of 1 μm. In this article we have presented an induction based differential coil system as a magnetic readout. The estimated theoretical limit of detection (LOD) is almost in the same sensitivity range as compared with commercial ELISA systems.

In summary, we have shown the development of a biomagnetic assay prototype using I) RCA coils and functional magnetic nanoparticles and II) an induction differential coil method. The assay does not require multiple washing steps and will be fast (~1 h). We presently require a total assay time of about 1.5 h which will be improved in the future. We have also determined that our ACS magnetic readout reaches a theoretical estimated LOD in the range of 55 fM (or 11 attomole) of RNA molecules. This value is expected to be further improved.

In the future several approaches will be applied in order to improve the LOD, such as 1) increase the number of available binding sites per RCA coil in order to bind more MNPs per RCA coil, 2) use a smaller set of induction coils in the DynoMag system which would lead to a lower readout noise, 3) add an additional RCA step in the sample preparation procedure (circle-to-circle amplification) in order to further increase the number of the RCA coils (with the cost of an increased TAT), 4) change of MNP system with a higher particle effective magnetic moment in the multi-core structure that will consequently increase the susceptibility per MNP [14], and thus increase the signal drop for each MNP that binds to the RCA coils.

Acknowledgements

The work is supported through Swedish Foundation for Strategic Research (SSF) grant “FLU-ID” #SBE13-0125, the Knut and Alice

Wallenberg foundation, the Swedish Infrastructure for Micro- and Nanofabrication – Myfab and by the European Commission Framework Programme 7 under the NanoMag project (grant agreement no: 604448).

References

[1] Q.A. Pankhurst, N.T.K. Thanh, S.K. Jones, J. Dobson, Progress in applications of magnetic nanoparticles in biomedicine, J. Phys. D: Appl. Phys. D 42 (2009) 224001.
[2] K.M. Krishnan, Biomedical nanomagnetics: a spin through possibilities in imaging diagnostics, and therapy, IEEE Trans. Magn. 46 (2010) 2523.
[3] K. Enpuku, Y. Tamai, T. Mitake, T. Yoshida, M. Matsuo, AC susceptibility measurement of magnetic markers in suspension for liquid phase immunoassay, J. Appl. Phys. 108 (2010) 034701.
[4] A.P. Astalan, F. Ahrentorp, C. Johansson, K. Larsson, A. Krozer, Biomolecular reactions studied using changes in Brownian rotation dynamics of magnetic particles, Biosens. Bioelectron. 19 (8) (2004) 945.
[5] M. Strömberg, J. Göransson, K. Gunnarsson, M. Nilsson, P. Svedlindh, M. Strømme, Sensitive molecular diagnostics using volume-amplified magnetic nanobeads, Nano Lett. 8 (3) (2008) 816–821.
[6] F.W. Østerberg, G. Rizzi, T. Zardán G.ómez de la Torre, M. Strömberg, M. Strømme, P. Svedlindh, M.F. Hansen, Measurements of Brownian relaxation of magnetic nanobeads using planar Hall effect bridge sensors, Biosens. Bioelectron. 40 (2013) 147 (15).
[7] I. Hsing, Y. Xu, W. Zhao, Micro- and Nano- magnetic particles for applications in biosensing, Electroanalysis 19 (7–8) (2007) 755–768.
[8] I. Koh, L. Josephson, Magnetic Nanoparticle Sensors, Sensors 9 (2009) 8130–8145.
[9] T. Zardan G.ómez de la Torre, A. Mezger, D. Herthnek, C. Johansson, P. Svedlindh, M. Nilsson, M. Strømme, Detection of rolling circle amplified DNA molecules using probe-tagged magnetic nanobeads in a portable AC susceptometer, Biosens. Bioelectron. 29 (1) (2011) 195.
[10] M. Nilsson, H. Malmgren, M. Samiotaki, M. Kwiatkowski, B.P. Chowdhary, U. Landegren, Circularizing oligonucleotides for localized DNA detection, Science 265 (1994) 2085–2088.
[11] F. Öisjöen, J.F. Schneiderman, A.P. Astalan, A. Kalabukhov, C. Johansson, D. Winkler, A new approach for bioassays based on frequency- and time-domain measurements of magnetic nanoparticles, Biosens. Bioelectron. 25 (5-5) (2010) 1008.
[12] S. Bogren, A. Fornara, F. Ludwig, M.P. Morales, U. Steinhoff, M.F. Hansen, O. Kazakova, C. Johansson, Classification of magnetic nanoparticle systems—synthesis, standardization and analysis methods in the nanomag project, Int. J. Mol. Sci. 16 (2015) 20308.
[13] F. Ludwig, O. Kazakova, L. Fernández Barquín, A. Fornara, L. Trahms, U. Steinhoff, P. Svedlindh, E. Wetterskog, Q.A. Pankhurst, P. Southern, P. Morales, M.F. Hansen, C. Frandsen, E. Olsson, S. Gustafsson, N. Gehrke, T. Buzug, M. Gräser, C. Grüttner, C. Jonasson, C. Johansson, Magnetic, structural and particle size analysis of single- and multi-core magnetic nanoparticles, IEEE Trans. Mag. 50 (11) (2014).
[14] F. Ahrentorp, A. Astalan, J. Blomgren, C. Jonasson, E. Wetterskog, P. Svedlindh, A. Lak, F. Ludwig, L.J. van IJzendoorn, F. Westphal, C. Grüttner, N. Gehrke, S. Gustafsson, E. Olsson, C. Johansson, Effective particle magnetic moment of multi-core particles, J. Magn. Magn. Mater. 380 (2015) 221.